MO Calculations on Sign and Magnitude of the Metal Spin Density in Alkali Radical Ion Pairs — Source link ⧉

G.W. Canters, C. Corvaja, E. de Boer

Related papers:

- Electron spin resonance studies of ion association between alkali metals ions and hydrocarbon radical ions

- Signs of alkali metal splittings and the structures of ion pairs of radical ions

- N.M.R. investigations on the alkali naphthalene ion pairs

- Association Between Sodium and Naphthalenide Ions1

- Charge Transfer in the Metal-Ligand Bond as Determined by Electron Spin Resonance

MO Calculations on Sign and Magnitude of the Metal Spin Density in Alkali Radical Ion Pairs*

GEE W. CANTERS

Department of Chemistry, University of North Carolina, Chapel Hill, North Carolina 27514

AND

C. CORVAJA†‡ AND E. DE BOER

Department of Physical Chemistry, University of Nijmegen, Nijmegen, The Netherlands

(Received 5 October 1970)

Formulas for the spin density at the metal nucleus in alkali radical ion pairs are derived by means of molecular orbital theory combined with first order perturbation theory. The formulas have been used for computer calculations of the metal spin density in the Na naphthalene (NaNl) ion pair. The results show that the zero- and first-order contributions to the metal spin density are of the same order of magnitude, but have different signs, and that the sign of the total spin density at the Na nucleus varies with the position of the Na ion in the ion pair. The experimentally observed dependence of the sign of the alkali coupling constant upon the atomic number of the metal is related to the difference in polarizing influence exerted by small and large ions on the π MO's of the aromatic ion. The temperature dependence of the metal coupling constant is explained by taking into account the change in the average position or the root-mean-square position of the alkali ion with a change in temperature.

I. INTRODUCTION

In 1961, Atherton and Weissman inferred from their ESR experiments on solutions of Na naphthalene (NaNl) that a certain amount of unpaired electron spin density was present at the alkali nucleus in the NaNl ion pair.[1] Since then, similar phenomena have been observed for numerous other systems. In 1965, De Boer proposed, on the basis of ESR experiments on Cs pyracene, that this spin density could be positive as well as negative and that sometimes a change in sign could occur with a change in temperature.[2] Later a number of systems was found in which a similar change in sign seemed to occur.[3] The existence of positive and negative metal spin densities was proven recently by NMR experiments,[4–8] and for a few systems a change in sign was indeed observed.[4,8] Two trends seemed to emerge from the NMR data. First, the metal hyperfine splitting constant (hfsc) showed a tendency to become negative with increasing atomic number,[6,8] a conclusion which was predicted at the same time by others on the basis of ESR data.[9] Second, a decrease in temperature was often found to be accompanied by a decrease in the magnitude of the metal hfsc, sometimes resulting in a change in sign from positive to negative.[4–6,8] Several models have been proposed to explain the existence of a nonzero spin density at the metal nucleus and, in a few cases, they have been worked out in detail.

Atherton and Weissman originally suggested that mixing of s orbitals of the metal with π orbitals of the aromatic ion might produce metal spin densities of the correct order of magnitude.[1] They did not consider the possibility of negative metal spin densities and no detailed calculations were reported. They described the dependence of the metal hfsc on the temperature by considering the vibration the alkali metal presumably performs in the potential well of the ion pair and the dependence of the amplitude of this vibration upon the temperature. Other models, based on earlier theories of Winstein and Grunwald,[10] were proposed to explain the temperature dependence of the metal hfsc: Hirota and Kreilick explained their ESR data by assuming the existence of an equilibrium between solvent separated and contact ion pairs in which the value of the metal hfsc would be different.[11a] Hogen-Esch and Smid used the same model to explain their uv data.[11b] On the other hand, NMR data obtained for Cs biphenyl in diglyme[5] could only be explained on the basis of the "static" model of Chang, Slates, and Szwarc.[11c]

Aono and Oohashi performed calculations on NaNl on the basis of a charge transfer model and also calculated the temperature dependence of the Na hfsc, a, by using the vibrational model of Atherton and Weissman.[12] The slope they calculated for the a vs T curve, however, although of the correct order of magnitude, turned out to be smaller than the experimentally measured slopes. They also indicated that in some systems bonding of the alkali ion with the σ-electron system of the radical might produce nonzero metal hfsc's. An example of such a system was recently investigated by the NMR method.[7]

To explain the occurrence of negative metal hfsc, De Boer considered positions of the metal ion in the nodal plane of the first antibonding molecular orbital (MO) of the aromatic π system.[2] For such a position, the zero order spin density vanishes and first order—possibly negative—contributions become important. He argued that the admixture of metal p orbitals into the π MO's of the aromatic ion might produce a negative spin density at the metal through core polarization. For the explanation of the temperature dependence of the metal hfsc, he used the vibrational model of Atherton and Weissman.

Pedersen and Griffin performed an INDO calculation for LiNl. They found negative spin densities for short distances between the Li and the Nl ion, but ran into convergence problems for larger distances.[13] The dependence of the Li hfsc on the position of the Li ion in the ion pair seemed to be consistent with an explanation of the temperature dependence of the metal hfsc on the basis of the vibrational model.

The most elaborate calculations up till now were reported by Goldberg and Bolton for different alkali Nl systems.[14] They performed a Hückel–McClelland MO calculation, accounting for the polarization of the π MO's by the metal ion, and they considered the admixture of the metal valence s orbital into the first antibonding MO of the Nl. However, since they performed only a zero order calculation, they were unable to account for negative spin densities.

In this article we consider ion pairs in which the radical anion is a planar π system. The case that the alkali ion is bonded to the σ-electron system of the radical is not considered since the mechanism which produces spin density at the metal nucleus in this situation seems to be well understood.[7,12,15] General formulas for the metal spin density will be presented in Sec. II. They are derived by means of MO theory and first-order perturbation theory. It is shown that De Boer's original explanation for the occurrence of negative metal spin densities is not valid. The formulas are applied to the special case of a NaNl ion pair and the expressions for the Na hfsc which were used for the computer calculations are given. Details about the calculations and the approximations used are presented in Sec. III and the results are presented and discussed in Sec. IV. On the basis of these results, the dependence of the sign of the metal hfsc upon the atomic number of the alkali nucleus and the dependence of magnitude and sign of the hfsc upon temperature are discussed. Finally, a few conclusions are presented in Sec. V.

II. THEORY

For the description of the wave function of the ion pair, we use as MO's linear combinations of carbon $2p_z$ atomic orbitals (AO's), $\{\chi_i\}$, denoted by Latin subscripts and AO's of the alkali metal, $\{\chi_\nu\}$, denoted by Greek subscripts. The AO, χ_i, is centered on the carbon atom C_i of the aromatic molecule. We assume that the MO's have been obtained from a variational calculation with a one electron Hamiltonian $\mathcal{3C}$, so that they are orthogonal and that, as the interaction between metal ion and aromatic ion will usually be small, the MO's, apart from a normalization constant, may be presented by

$$\Phi_i = \Phi_i^0 + \sum_\nu c_\nu^i \chi_\nu, \tag{1a}$$

$$\Phi_\mu = \chi_\mu + \sum_j c_j^\mu \Phi_j^0. \tag{1b}$$

Here Φ_i^0 represents a π MO of the free aromatic ion, and the c_ν^i and c_j^μ are mixing constants. The MO's of the ion pair thus closely resemble those of the free ions. The MO's, $\{\Phi_i\}$ and $\{\Phi_\nu\}$, will be called "aromatic" and "metallic" MO's, respectively. In subscripting the MO's, the following conventions are used. The m-bonding MO's of the aromatic ion are denoted by $\Phi_1^0, \cdots,$ Φ_m^0, and the first antibonding MO by Φ_{m+1}^0. The core AO's of the metal are denoted by $\chi_{1s}, \cdots, \chi_\xi$, and the valence AO's by χ_{ns}, χ_{np}, etc. An arbitrary MO, either metallic or aromatic, which is doubly occupied in the zero-order ground state of the ion pair will be denoted by Φ_z and an arbitrary empty MO by Φ_y.

The zero order ground state wavefunction of the ion pair, corresponding to the configuration Ar⁻Me⁺, in which Ar and Me denote, respectively, the aromatic molecule and the metal atom, can now be presented by the Slater determinant

$$^2\Psi_0 = [1/(N!)^{1/2}] \, | \, \Phi_1 \bar{\Phi}_1 \cdots \Phi_m \bar{\Phi}_m \Phi_{m+1} \Phi_{1s} \bar{\Phi}_{1s} \cdots \Phi_\xi \bar{\Phi}_\xi \, |, \tag{2}$$

in which N is the number of electrons described by the wavefunction. An MO without a bar describes an electron with an α spin and an MO with a bar an electron with a β spin. Taking into account electron correlation results in an improved ground state wavefunction $^2\Psi$ which, apart from a normalization constant, is given by

$$^2\Psi = {}^2\Psi_0 + \sum_i \lambda_i \, {}^2\Psi_i. \tag{3}$$

The summation over i runs over all the excited doublet wavefunctions $^2\Psi_i$, which are linear combinations of Slater determinants. The mixing coefficients λ_i can be calculated by perturbation theory with the use of the perturbation Hamiltonian $\mathcal{3C}^1$, defined by

$$\mathcal{3C}^1 \equiv \sum_{i>j} (e^2/r_{ij}). $$

Here r_{ij} is the distance between electrons i and j, e is the electric charge of an electron and the summation is over all pairs of electrons. The spin density $\rho(\mathbf{r}_N)$ at the metal nucleus is given by the expectation value of the spin density operator $\rho_{op}(\mathbf{r}_N)$, in which $\mathbf{r}_N$ is the radius vector of the metal nucleus. $\rho_{op}(\mathbf{r})$ is defined by[16]

$$\rho_{op}(\mathbf{r}) \equiv M_z^{-1} \sum_i S_{z,i} \delta(\mathbf{r}_i - \mathbf{r}), \tag{4}$$

in which $S_{z,i}$ is the operator for the z component of the angular momentum of electron i, $M_z \equiv \langle \sum_i S_{z,i} \rangle$, $\delta(\mathbf{r})$ is the Dirac delta function and $\mathbf{r}_i$ is the radius vector of electron i. The summations over i run over all the ectelrons in the wavefunction. Using the Eqs. (3) and

(4) the expression for $\rho(\mathbf{r}_N)$ becomes

$$\rho(\mathbf{r}_N) = \langle {}^2\Psi_0 \mid \rho_{op}(\mathbf{r}_N) \mid {}^2\Psi_0 \rangle$$
$$+ 2 \sum_i \lambda_i \mid \langle {}^2\Psi_0 \mid \rho_{op}(\mathbf{r}_N) \mid {}^2\Psi_i \rangle \mid$$
$$+ \sum_i \sum_j \lambda_i \lambda_j \langle {}^2\Psi_i \mid \rho_{op}(\mathbf{r}_N) \mid {}^2\Psi_j \rangle. \quad (5)$$

A wavefunction can be characterized by the number of singly occupied MO's in the Slater determinants of which it is built. A wavefunction $\mid n \rangle$ of type n will have $2n+1$ singly occupied MO's in its Slater determinants; ${}^2\Psi_0$ will be represented by $\mid 0 \rangle$, and the other wavefunctions of type 0 by $\mid 0' \rangle$. Since $\rho_{op}(\mathbf{r})$ is a sum of one electron operators, $\langle n \mid \rho_{op}(\mathbf{r}) \mid m \rangle \equiv 0$, unless $n - m = -1$, 0 or 1. Therefore, if in Eq. (5) the terms quadratic in the λ's are neglected, only terms like $\langle 0 \mid \rho_{op}(\mathbf{r}_N) \mid 0 \rangle$, $\langle 0 \mid \rho_{op}(\mathbf{r}_N) \mid 0' \rangle$, and $\langle 0 \mid \rho_{op}(\mathbf{r}_N) \mid 1 \rangle$ remain. They are discussed below:

(1) From the Eqs. (2) and (4), one finds for the first term of Eq. (5)

$$\langle 0 \mid \rho_{op}(\mathbf{r}_N) \mid 0 \rangle = \mid \Phi_{m+1}(\mathbf{r}_N) \mid^2 \geq 0.$$

(2) Since $\rho_{op}(\mathbf{r})$ is a sum of one electron operators, it follows that $\langle 0 \mid \rho_{op}(\mathbf{r}_N) \mid 0' \rangle \equiv 0$ unless the Slater determinants representing $\mid 0 \rangle$ and $\mid 0' \rangle$ differ in only one MO. Therefore, we only need to consider wavefunctions $\mid 0' \rangle$ which can be obtained from ${}^2\Psi_0$ by exciting an electron from a doubly occupied MO Φ_x into Φ_{m+1} or by exciting the unpaired electron out of Φ_{m+1} into an empty MO Φ_y. The wavefunctions belonging to the corresponding excited states will be denoted by ${}^2\Psi_{x,m+1}$ and ${}^2\Psi_{m+1,y}$, respectively, and the corresponding λ's by $\lambda_{x,m+1}$ and $\lambda_{m+1,y}$. The sum of the contributions from these excitations to $\rho(\mathbf{r}_N)$ together with the term $\langle 0 \mid \rho_{op}(\mathbf{r}_N) \mid 0 \rangle$ discussed above will be denoted by

ρ_0. ρ_0 is approximately given by

$$\rho_0 \approx \mid \Phi_{m+1}(\mathbf{r}_N) + \sum_x \lambda_{x,m+1} \Phi_x(\mathbf{r}_N)$$
$$+ \sum_y \lambda_{m+1,y} \Phi_y(\mathbf{r}_N) \mid^2 \geq 0, \quad (6)$$

in which the summations over x and y run over the doubly occupied and empty MO's of the ion pair in the zero orderground state, respectively. The error made in this approximation is quadratic in the λ's and is probably small. According to first-order perturbation theory, $\lambda_{x,m+1}$ and $\lambda_{m+1,y}$ are given by

$$\lambda_{x,m+1} = \sum_{i=1}^{m+1} \frac{2[ii \mid x\, m+1] - [ix \mid m+1\, i]}{E_{m+1} - E_x}, \quad (7a)$$

$$\lambda_{m+1,y} = \sum_{i=1}^{m} \frac{2[ii \mid y\, m+1] - [iy \mid m+1\, i]}{E_{m+1} - E_y}, \quad (7b)$$

in which E_k is the zero-order energy of the MO Φ_k. The integrals $[ij \mid kl]$ which occur in the Eqs. (7) are defined by

$$[ij \mid kl] \equiv \int \Phi_i^*(1) \Phi_k^*(2) (e^2/r_{12}) \Phi_j(1) \Phi_l(2) d\mathbf{r}_1 d\mathbf{r}_2. \quad (8)$$

Equation (6) shows that excitations producing states of the type $\mid 0' \rangle$ can probably not produce negative metal spin densities.

(3) As was done for the terms $\langle 0 \mid \rho_{op}(\mathbf{r}_N) \mid 0' \rangle$, it can be shown that for the evaluation of the elements $\langle 0 \mid \rho_{op}(\mathbf{r}_N) \mid 1 \rangle$ only configurations $\mid 1 \rangle$ need to be considered which are obtained from ${}^2\Psi_0$ by exciting an electron from a doubly occupied MO Φ_x into an empty MO Φ_y. The wavefunction corresponding to the excitation $x \to y$ for which $\langle 0 \mid \rho_{op}(\mathbf{r}_N) \mid 1 \rangle \neq 0$ is denoted by ${}^2\Psi_{x,y}$ and is given by

$${}^2\Psi_{x,y} = (6)^{-1/2} \{ [2/(N!)^{1/2}] \mid \cdots \Phi_k \bar{\Phi}_k \cdots \Phi_{m+1} \Phi_x \Phi_y \cdots \Phi_\nu \bar{\Phi}_\nu \cdots \mid - (N!)^{-1/2} \mid \cdots \Phi_k \bar{\Phi}_k \cdots \Phi_{m+1} \bar{\Phi}_x \Phi_y \cdots \Phi_\nu \bar{\Phi}_\nu \cdots \mid$$
$$- (N!)^{-1/2} \mid \cdots \Phi_k \bar{\Phi}_k \cdots \Phi_{m+1} \Phi_x \bar{\Phi}_y \cdots \Phi_\nu \bar{\Phi}_\nu \cdots \mid \}. \quad (9)$$

The corresponding mixing coefficient in Eq. (3) is denoted by $\lambda_{x,y}$ and, according to first order perturbation theory, is given by

$$\lambda_{x,y} = \frac{1}{2}(6)^{1/2} \{ [m+1\, x \mid y\, m+1]/(E_y - E_x) \}. \quad (10)$$

The corresponding contribution to the spin density, which will be denoted by $\rho_{x,y}$, is given by

$$\rho_{x,y} = [4/(6)^{1/2}] \lambda_{x,y} \mid \Phi_x(\mathbf{r}_N) \Phi_y(\mathbf{r}_N) \mid, \quad (11)$$

and the sum of these contributions is denoted by ρ_1 and can be presented by the following expression

$$\rho_1 = \sum_x \sum_y \rho_{x,y} = [4/(6)^{1/2}] \sum_x \sum_y \lambda_{x,y} \mid \Phi_x(\mathbf{r}_N) \Phi_y(\mathbf{r}_N) \mid. \quad (12)$$

Here, the summations over x and y run over the doubly

occupied and the empty MO's of the ion pair in the ground state, respectively. The calculation of ρ_1 can be simplified by considering the elements $\rho_{x,y}$ in more detail. Starting points for the following discussion are the Eqs. (10) and (12).

In the beginning of this section, the MO's were divided into aromatic and metallic MO's. Consequently, the $\rho_{x,y}$ can be divided in four categories.

A. Local Metal Excitations

The first category derives from excitations $x \to y$ in which Φ_x and $\dot{\Phi}_y$ are a doubly occupied metallic MO Φ_ν and an empty metallic MO Φ_μ, respectively. They correspond to configurations $Ar^-(Me^+)^*$ in which the metal ion is in an excited state. The contribution of these excitations to ρ_1 is denoted by ρ_M and, according

TABLE I. Isotropic hyperfine splitting constants for the free alkali atoms in the n^2S and n^2P state.

	^{6}Li	^{7}Li	^{23}Na	^{39}K	^{85}Rb	^{87}Rb	^{133}Cs
$A(n^2S) \times h^{-1}$, Mc/sec	152.1	401.8	886	231	1012	3417	2298
$A(n^2P) \times h^{-1}$, Mc/sec[a]	−10.9	−28.7	−0.5[b]	−0.2[b]	2	8	28

[a] Apart from Cs no relativistic or volume corrections have been applied to calculate $A(n^2P)$.

[b] The sign of $A(n^2P)$ is uncertain; see the Appendix. The following references were used in the calculation of $A(n^2S)$ and $A(n^2P)$: $A(n^2S)$: P. Kusch and H. Taub, Phys. Rev. **75**, 1477 (1949). $A(n^2P)$: Li: K. C. Brog, T. G. Eck, and H. Wieder, Phys. Rev. **153**, 91 (1967); G. J. Ritter, Can. J. Phys. **43**, 770 (1965); J. D. Lyons, R. T. Pu, and T. P. Das, Phys. Rev. **178**, 103 (1969). Na: M. L. Perl, I. I. Rabi, and B. Senitzky, Phys. Rev. **98**, 611 (1955); J. N. Dodd and R. W. N. Kinnear, Proc. Phys. Soc. (London) **75**, 51 (1960); H. Ackermann, Z. Phys. **194**, 253 (1966); M. Baumann, W. Hartmann, H. Krüger, and A. Oed, *ibid.* **194**, 270 (1966); M. Baumann, Z. Naturforsch. **24a**, 1049 (1969). K: P. Buck and I. I. Rabi, Phys. Rev. **107**, 1291 (1957). Rb: B. Senitzky and I. I. Rabi, Phys. Rev. **103**, 315 (1956); H. A. Schüssler, Z. Phys. **182**, 289 (1965). Cs: S. Svanberg and S. Rydberg, Z. Phys. **227**, 216 (1969).

to Eqs. (10) and (12), is given by

$$\rho_M = \sum_\nu \sum_\mu \rho_{\nu,\mu} = 2 \sum_\nu \sum_\mu \{[m+1\, \nu \mid \mu\, m+1]/(E_\mu - E_\nu)\}$$
$$\times \mid \Phi_\nu(\mathbf{r}_N) \Phi_\mu(\mathbf{r}_N) \mid.$$

To simplify this expression, $\Phi_\nu(\mathbf{r}_N) \Phi_\mu(\mathbf{r}_N)$ is replaced by $\chi_\nu(\mathbf{r}_N) \chi_\mu(\mathbf{r}_N)$ and $E_\mu - E_\nu$ by $\Delta E_{\nu,\mu}$, which is the energy difference between the AO's χ_ν and χ_μ in the free metal atom. Furthermore, for the evaluation of the integral $[m+1\, \nu \mid \mu\, m+1]$, we only consider the admixture of χ_{ns} and χ_{np}—which are valence AO's of the metal—into Φ_{m+1}. The errors involved in these replacements are small. In this way the expression for ρ_M becomes

$$\rho_M = 2 \mid c_{ns}{}^{m+1} \mid^2 \sum_\nu \sum_\mu [(ns\, \nu \mid \mu\, ns)/\Delta E_{\nu,\mu}]$$
$$\times \mid \chi_\nu(\mathbf{r}_N) \chi_\mu(\mathbf{r}_N) \mid$$
$$+ 2 \mid c_{np}{}^{m+1} \mid^2 \sum_\nu \sum_\mu [(np\, \nu \mid \mu\, np)/\Delta E_{\nu,\mu}]$$
$$\times \mid \chi_\nu(\mathbf{r}_N) \chi_\mu(\mathbf{r}_N) \mid. \quad (13)$$

The integrals $(pq \mid rs)$ which occur in this expression are defined by

$$(pq \mid rs) \equiv \int \chi_p{}^*(1) \chi_r{}^*(2) (e^2/r_{12}) \chi_q(1) \chi_s(2)\, d\mathbf{r}_1 d\mathbf{r}_2.$$

The first and the second sum in Eq. (13) represent the contribution to the metal spin density from the polarization of the metal core by the unpaired electron through the admixture of χ_{ns} and χ_{np}, respectively, in Φ_{m+1}.

The first sum in Eq. (13) can be compared with the spin density caused by the unpaired valence electron through core polarization in the n^2S state of the free atom. Goodings has shown[17] that for Li, Na, and K this spin density is positive and amounts to 20%–30% of the spin density caused directly by the ns electron through the Fermi contact interaction. This part of ρ_M, therefore, can never give rise to negative spin densities. Instead of calculating it in detail, it is more convenient to take core polarization terms of this type into account in a semiempirical way by adjusting the parameter used in the conversion of spin densities into coupling constants. This will be discussed in Sec. III.

Terms of the type occurring in the second sum of Eq. (13) were originally held responsible for the occurrence of negative spin densities.[2] As mentioned in the Introduction, this assumption is not granted by a more detailed analysis. This can be seen as follows. The second sum in Eq. (13) can be compared with the spin density at the metal nucleus $\rho(n^2P)$ when the free atom is in the n^2P state. $\rho(n^2P)$ can be calculated from the hfsc in the n^2P state, $A(n^2P)$, from the expression[18]

$$A(n^2P) = \tfrac{3}{8}\pi \gamma_e \gamma_N \hbar^2 \rho(n^2P), \quad (14)$$

in which γ_e and γ_N denote the gyromagnetic constants of the electron and the alkali nucleus, respectively, $\hbar$ is the constant of Planck divided by 2π and $A(n^2P)$ is given in energy units. Values of $A(n^2P)$ can be obtained from spectroscopic data as explained in the Appendix. Together with values of $A(n^2S)$, the hfsc in the n^2S state of the free alkali atom, they are presented in Table I for different alkali isotopes. The data in this table show that, apart from Li, the absolute value of the spin density at the metal nucleus due to core polarization by an np electron is less than 1% of the spin density brought about by an ns electron. Moreover, the sign of this contribution changes from negative for Li to positive for Rb and Cs, which is contrary to the trends observed experimentally for the ion pairs as was stated in the Introduction. The second sum in Eq. (13) will therefore be neglected. In conclusion, one can say that ρ_M will be positive and that its contribution to the total spin density can be accounted for semiempirically. For this reason ρ_M has been omitted from the final expression for ρ_1.

B. Local Aromatic Excitations

The second category of contributions to ρ_1 derives from so-called local aromatic excitations, $x \rightarrow y$, in which both x and y denote aromatic MO's. They are the complement of the local metal excitations discussed in the preceding paragraph and correspond to configurations $(Ar^-)^*Me^+$ in which the aromatic ion is in an excited state. The sum of the contributions of this type will be denoted by ρ_{Ar} and, according to the

Eqs. (10) and (12), is given by

$$\rho_{Ar} = \sum_i \sum_j \rho_{ij} = 2 \sum_i \sum_j \{[m+1\,i\,|\,j\,m+1]/(E_j - E_i)\}$$
$$\times |\Phi_i(\mathbf{r}_N)\Phi_j(\mathbf{r}_N)|. \quad (15)$$

The summations over i and j run over the doubly occupied and the empty MO's, respectively, of the ion pair in the ground state. Unless the admixture of s orbitals of the metal in the aromatic MO's is large, one expects ρ_{Ar} to be small. However, detailed calculations are needed to evaluate sign and magnitude of ρ_{Ar}. Results of these calculations are reported in Sec. IV.

The two remaining categories of excitations are so-called "cross excitations," by which an electron is excited out of an aromatic into a metallic MO or vice versa. They correspond to charge transfer (CT) states, and take into account the cross correlation between electrons in different moieties of the ion pair.

C. Aromatic–Metal Cross Excitations

Excitations of an electron out of a doubly occupied aromatic MO Φ_i into an empty metallic MO Φ_μ produce CT states Ar*Me or Ar*Me* in which the aromatic molecule or the aromatic molecule as well as the metal atom is in an excited state. Their total contribution to ρ_1 will be denoted by $\rho_{Ar,M}$. According to the Eqs. (10) and (12) $\rho_{Ar,M}$ is given by

$$\rho_{Ar,M} = \sum_i \sum_\mu \rho_{i,\mu} = 2 \sum_i \sum_\mu \{[m+1\,i\,|\,\mu\,m+1]/(E_\mu - E_i)\}$$
$$\times |\Phi_i(\mathbf{r}_N)\Phi_\mu(\mathbf{r}_N)|, \quad (16)$$

in which the summations over i and μ run over the doubly occupied aromatic MO's and the empty metallic MO's respectively, of the ion pair in the ground state. Since the spin density at the metal nucleus in a CT state like Ar*Me is large, one expects excitations of this type to provide for a substantial contribution to ρ_1. The sign of $\rho_{Ar,M}$ can possibly be inferred from a consideration of the contribution to $\rho_{Ar,M}$ from a particular excitation $i \rightarrow ns$. From the Eqs. (1) and (16), it follows that an important term in the expression for this contribution $\rho_{i,ns}$ will be the term

$$2c_i^{ns}\{[m+1\,i\,|\,i\,m+1]/(E_{ns} - E_i)\}c_{ns}^i\,|\,\chi_{ns}(\mathbf{r}_N)\,|^2.$$

Since the integral will be positive, as will $E_{ns} - E_i$, and since c_{ns}^i and c_i^{ns} will have different signs, this term will be negative. One expects, therefore, $\rho_{Ar,M}$ usually to be negative. Results of calculations on $\rho_{Ar,M}$ are reported in Sec. IV.

D. Metal–Aromatic Cross Excitations

Excited configurations which are obtained from the zero-order ground state configuration by exciting an electron from a doubly occupied metallic MO Φ_ν into an empty aromatic MO Φ_j correspond to CT states $(Ar^-)^*Me^{++}$ and $(Ar^-)^*(Me^{++})^*$, in which the aromatic ion or the aromatic ion as well as the metal ion is

in an excited state. Since the metallic MO's Φ_ν are core type MO's, which are strongly contracted, the overlap between the metal AO χ_ν and the pure aromatic MO Φ_j^0 will be small and consequently, their mixing will be small. In addition, $\lambda_{\nu,j}$ will be small due to the large difference between E_ν and E_j (e.g., the first ionization potential of Na amounts to 5.14 eV while the second ionization potential amounts to 47.3 eV[19]). On the other hand, the contraction of core s orbitals will provide for a large probability amplitude of χ_ν at the nucleus. The latter two effects (large energy difference and large density of core s AO's at the nucleus) also play a role in the local metal excitations discussed above. The overlap effect, however, does not play a role in the local metal excitations, but it does affect the elements $\rho_{\nu,j}$, making their total contribution probably smaller than ρ_M. Therefore, the effect of metal–aromatic cross excitations on the spin density has been neglected.

The results of the preceding discussion can be summarized and simplified as follows:

(a) The total spin density at the metal nucleus, $\rho(\mathbf{r}_N)$, is given by

$$\rho(\mathbf{r}_N) = \rho_0 + \rho_1. \quad (17)$$

The zero order spin density, ρ_0, is ≥ 0 and is given by the Eqs. (6) and (7). The first-order spin density, ρ_1, is given by

$$\rho_1 = \rho_{Ar} + \rho_{Ar,M} \quad (18)$$

in which ρ_{Ar} and $\rho_{Ar,M}$ are given by the Eqs. (15) and (16), respectively.

(b) Of the complete set of AO's of the metal only the valence AO's and higher AO's need to be considered. Since only s orbitals have a nonzero probability density at the nucleus and since, of these s AO's, the valence AO will show the largest mixing with the MO's Φ_i^0, only this AO will be considered in the calculations. The expressions for the aromatic and metallic MO's then reduce to [cf. the Eqs. (1)]

$$\Phi_i = \Phi_i^0 + c_{ns}^i\,\chi_{ns}, \quad (19a)$$

$$\Phi_{ns} = \chi_{ns} + \sum_i c_i^{ns}\,\Phi_i^0. \quad (19b)$$

Finally, for $\Phi(\mathbf{r}_N)$ and $\Phi_{ns}(\mathbf{r}_N)$, the following simplified expressions will be used:

$$\Phi_i(\mathbf{r}_N) = c_{ns}^i\,\chi_{ns}(\mathbf{r}_N), \quad (20a)$$

$$\Phi_{ns}(\mathbf{r}_N) = \chi_{ns}(\mathbf{r}_N), \quad (20b)$$

which means that the terms $\Phi_i^0(\mathbf{r}_N)$ have been neglected. This is justified because, for instance, for Li, Na, and K, even for a C–Me distance as short as 2 Å, the density of a carbon $2p_z$-AO at the metal nucleus is about three orders of magnitude smaller than $|\chi_{ns}(\mathbf{r}_N)|^2$.

In the next paragraph Eqs. (6), (7), and (15)–(20) will be evaluated for the case of a Na naphthalene (NaNl) ion pair.

E. Application to a NaNl Ion Pair

The molecular axis system used in the calculations on NaNl is shown in Fig. 1. To simplify the discussions and the calculations, we consider only positions of the Na nucleus in the XZ plane. This has the advantage that the ion pair has at least C_s symmetry, which allows one to restrict the number of excitations to be taken into account on the basis of symmetry considerations. The bonding MO's of pure Nl are denoted by $\Phi_1{}^0, \cdots,$ $\Phi_5{}^0$; the antibonding MO's by $\Phi_6{}^0, \cdots, \Phi_{10}{}^0$. $\Phi_6{}^0$ is the first antibonding MO. The symmetries of these MO's are given in Table II. The valence s AO of Na will be denoted by χ_{3s}. In the following, the expressions for ρ_0 and ρ_I are given.

F. Zero Order Spin Density ρ_0

Symmetry arguments show that, apart from the ground state configuration $^2\Psi_0$, the only configurations to be considered for the calculation of ρ_0 derive from the excitations $1\rightarrow6$, $4\rightarrow6$, $6\rightarrow8$, $2\rightarrow6$ and $6\rightarrow3s$. The first three excitations are expected to give small contributions to ρ_0, since the symmetries of the corresponding parent MO's ($\Phi_1{}^0$ and $\Phi_6{}^0$, $\Phi_4{}^0$ and $\Phi_6{}^0$, and $\Phi_6{}^0$ and $\Phi_8{}^0$, respectively) do not match; they are therefore neglected. According to Eq. (6) and (20), the expression for ρ_0 then becomes

$$\rho_0 = | c_{3s}{}^6 + \lambda_{2,6}c_{3s}{}^2 + \lambda_{6,3s} |^2 | \chi_{3s}(\mathbf{r}_N) |^2. \quad (21)$$

According to Eq. (7), $\lambda_{2,6}$ and $\lambda_{6,3s}$ are given by

$$\lambda_{2,6} = \sum_{i=1}^{6} \frac{2[ii \mid 2\,6] - [i\,2 \mid 6\,i]}{E_6 - E_2}, \quad (22a)$$

$$\lambda_{6,3s} = \sum_{i=1}^{6} \frac{2[ii \mid 6\,3s] - [i\,6 \mid 3s\,i]}{E_6 - E_{3s}}. \quad (22b)$$

G. First-Order Spin Density ρ_1

According to Eq. (18), for the calculation of ρ_1, only ρ_{Ar} and $\rho_{Ar,M}$ need to be considered.

1. ρ_{Ar}

As was done for the calculation of ρ_0, one can show from symmetry arguments that the only excitations which may give a substantial contribution to ρ_{Ar} are the excitations $1\rightarrow8$ and $4\rightarrow8$. Thus, according to Eq. (15), ρ_{Ar} is given by

$$\rho_{Ar} = \rho_{1,8} + \rho_{4,8}, \quad (23)$$

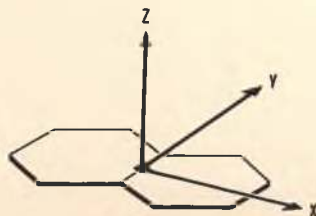and from the Eqs. (15) and (20), it follows that $\rho_{i,8}$

Fig. 1. Molecular axis system used in the calculations on NaNl.

TABLE II. Symmetries of the MO's $\Phi_i{}^0$ of pure Nl according to their representations in the groups D_{2h} and C_s.

MO	D_{2h}	C_s	MO	D_{2h}	C_s
1	B_{1u}	A'	6	B_{2g}	A'
2	B_{2g}	A'	7	B_{3g}	A''
3	B_{3g}	A''	8	B_{1u}	A'
4	B_{1u}	A'	9	A_u	A''
5	A_u	A''	10	B_{3g}	A''

$(i=1, 4)$ is given by

$$\rho_{i,8} = 2\{[6\,i \mid 8\,6]/(E_8 - E_i)\}c_{3s}{}^i c_{3s}{}^8 | \chi_{3s}(\mathbf{r}_N) |^2 \quad (24)$$

2. $\rho_{Ar,M}$.

In a similar way, one finds for $\rho_{Ar,M}$ from the Eqs. (16) and (20)

$$\rho_{Ar,M} = \rho_{1,3s} + \rho_{2,3s} + \rho_{4,3s}, \quad (25)$$

$$\rho_{i,3s} = 2\{[6\,i \mid 3s\,6]/(E_{3s} - E_i)\}c_{3s}{}^i | \chi_{3s}(\mathbf{r}_N) |^2$$
$$(i=1, 2, 4). \quad (26)$$

The Eqs. (21)–(26) were used to perform the computer calculations, of which the details are discussed in the next section.

III. DETAILS OF THE CALCULATIONS

In the following, the choice of MO's $\Phi_i{}^0$, the values chosen for the energies E_i and E_{3s}, the formulas and parameters used for the evaluation of $c_{3s}{}^i$ and $c_i{}^{3s}$, the calculation of the integrals $[ij \mid kl]$ and $[ij \mid k\,3s]$, and the value of the parameter used to convert spin densities into coupling constants are discussed. In addition, the evaluation of ρ_0 and details about the computer programs are discussed.

A. MO's $\Phi_i{}^0$ and Energies E_i and E_{3s}

For the MO's $\Phi_i{}^0$, Hückel MO's were used.[20] The energies E_i of the MO's Φ_i were set equal to the energies of the unperturbed MO's $\Phi_i{}^0$. For the energy of the MO $\Phi_s{}^0$ a value of -8.3 eV was used which is equal to the oxidation potential of neutral Nl.[21] The energies of the other MO's $\Phi_i{}^0$ were derived from this value by taking the Hückel energy difference between $\Phi_i{}^0$ and $\Phi_5{}^0$ into account and using for the Hückel resonance integral parameter β a value of -2.371 eV.[20,21] The energies E_i are given in Table III. A value for E_{3s} was obtained by setting the energy difference between Φ_6 and Φ_{3s} equal to the enthalpy ΔH of the reaction between atomic Na and Nl in solution

$$Na + Nl \rightarrow Na^+ Nl^-.$$
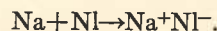
According to this definition, $E_6 - E_{3s} = \Delta H$. ΔH is given by[22]

$$\Delta H = E_{Nl} + I_{Na} + \Delta H_{solv} + Q, \quad (27)$$

TABLE III. Energies of the aromatic MO's Φ_i used in the calculations.

MO	E, eV	MO	E, eV
1	−12.293	6	−5.371
2	−10.670	7	−4.465
3	−9.923	8	−3.748
4	−9.205	9	−3.001
5	−8.300	10	−1.378

in which E_{N1} is the electron affinity of Nl, I_{Na} is the ionization potential of Na, ΔH_{solv} is the enthalpy change due to the change in solvation of the reactants, and Q is the Coulomb energy of the ions in the ion pair. ΔH_{solv} depends mainly on the solvation of the Na ion in the ion pair. The quantity $\Delta H'$, defined by

$$\Delta H' \equiv \Delta H + L_{Na},$$

in which L_{Na} is the sublimation energy of metallic Na, has been determined experimentally for a number of systems.[22] Since $L_{Na} = 1.013$ eV[22] and $E_6 = -5.371$ eV (see Table III), E_{3s} can be calculated directly from the equation

$$E_{3s} = -4.36 - \Delta H' \text{ eV}.$$

Since $\Delta H'$ varies with solvent, E_{3s} varies with solvent. A minimum of -4.36 eV for E_{3s} is found if $\Delta H' = 0$. On the other hand, in systems like Na+biphenyl in diethoxyethane (DEE), $\Delta H'$ may become as low as -0.95 eV.[22] One expects therefore that for NaNl in different solvents E_{3s} may vary from -4.4 eV to -3.3 eV. For NaNl in DEE, $\Delta H' = -0.52$ eV,[23] which is probably the reaction enthalpy for the formation of contact ion pairs. Using this value for $\Delta H'$, one finds $E_{3s} = -3.84$ eV. Apart from performing the calculations for $E_{3s} = -3.84$ eV, in the next section the variation of ρ_1 with E_{3s} will be considered. The calculation for $E_{3s} = -3.84$ eV has special significance, since for this value of E_{3s} χ_{3s} and Φ_8^0 are nearly degenerate, and it becomes of interest to see how ρ_1, ρ_{Ar} and $\rho_{Ar,M}$ are affected when appreciable mixing occurs between χ_{3s} and one of the antibonding MO's of Nl.

B. Coefficients $c_{3s}{}^i$ and $c_i{}^{3s}$

For the calculation of the coefficient $c_{3s}{}^i$ the following formula was used[24]

$$c_{3s}{}^i = (H_{i,3s} - E_i S_{i,3s})/(E_i - E_{3s}), \quad (28)$$

and a similar one was used for the calculation of $c_i{}^{3s}$. $S_{i,3s}$ is the overlap integral between Φ_i^0 and χ_{3s} and is given by

$$S_{i,3s} \equiv \langle \Phi_i^0 \mid \chi_{3s} \rangle$$

$$= \sum_{j=1}^{10} b_{ij} \langle \chi_j \mid \chi_{3s} \rangle$$

$$= \sum_{j=1}^{10} b_{ij} \cos\theta_j (2p_\sigma \mid 3s)_j,$$

in which the b_{ij} are the coefficients of the $2p_z$ AO's χ_j in the MO Φ_i^0, θ_j is the angle between the Z axis and the vector $\mathbf{r}_{j,N} \equiv \mathbf{r}_N - \mathbf{r}_j$, $\mathbf{r}_j$ being the radius vector of C atom C_j, and $(2p_\sigma \mid 3s)_j$ is the overlap integral for a $2p_\sigma$-orbital at C_j, and χ_{3s}. Values for $2p_\sigma \mid 3s)_j$ were calculated from the formulas given by Mulliken et al.[25] These formulas were used with values of 1.625 and 0.733 for the parameters μ_C and μ_{Na} occurring in these formulas.[25] For the calculation of the vectors $\mathbf{r}_j$ it was assumed that the carbon skeleton of Nl consists of two regular hexagons with distances between adjacent C atoms of 1.40 Å. $H_{i,3s}$ denotes the matrix element $\langle \Phi_i^0 \mid \mathcal{H} \mid \chi_{3s} \rangle$. According to Wolfsberg and Helmholz[26] these elements can be approximated by

$$H_{i,3s} = (F/2)(E_i + E_{3s})S_{i,3s}, \quad (29)$$

in which F is an adjustable parameter which must satisfy the condition $1 < F < 2$. Usually F is chosen between 1.8 and 2.0.[26] For our calculations, we used for F a value of 2.0. A change in F from 2.0 to 1.9 changed the values of a_1 by +0.2 to +0.3 G. Equation (28) is strictly valid only for a variational calculation with a basis set of two orbitals under the condition

$$\left| \tfrac{1}{2}(E_i + E_{3s})S_{i,3s} \right| \ll \left| E_i - E_{3s} \right|. \quad (30)$$

Although our basis set consists of 11 orbitals, Eq. (28) is still a good approximation due to the fact that the mixing of the MO's Φ_i^0 with each other under the influence of the Hamiltonian $\mathcal{H}$ is negligible. Condition (30) was always satisfied except for $E_{3s} = -3.84$ eV, in which case $c_{3s}{}^8$ and $c_8{}^{3s}$, as calculated from (28), differed by 10%–20% from the values calculated by solving the secular equations for Φ_8^0 and χ_{3s} exactly. However, this occurred only for a few positions of the Na ion, for which $S_{8,3s}$ reached a maximum.

C. Integrals $[ij \mid kl]$ and $[ij \mid k \, 3s]$

Integrals $[ij \mid kl]$ were calculated by replacing MO's Φ_n by Φ_n^0. In this way, the integral $[ij \mid kl]$ becomes a sum of integrals $(pq \mid rs)$. These integrals were evaluated by using the zero differential overlap (ZDO) approximation.[27,28] Values for the integrals $(pp \mid qq)$ were taken from Table I of Ref. (20).

Integrals $[ij \mid k \, 3s]$ are approximately given by

$$[ij \mid k \, 3s] \approx c_{3s}{}^k [ij \mid 3s3s]^0 + \sum_{l=1}^{10} c_l{}^{3s} [ij \mid kl]^0, \quad (31)$$

in which the zero superscripts at the integrals indicate that the MO's $\Phi_i \cdots \Phi_l$ and Φ_{3s} have been replaced by $\Phi_i^0 \cdots \Phi_l^0$ and χ_{3s}, respectively. Evaluation of the second term proceeds as indicated before. In the ZDO approximation the integral $[ij \mid 3s3s]^0$ is a sum of integrals $(2p_z 2p_z \mid 3s3s)$ which can be evaluated according to the equation

$$(2p_z 2p_z \mid 3s3s) = (\pi\pi \mid 3s3s) \sin^2\theta + (\sigma\sigma \mid 3s3s) \cos^2\theta.$$

$(\pi\pi \mid 3s3s)$ and $(\sigma\sigma \mid 3s3s)$ are Coulomb repulsion integrals between a Na 3s orbital and a carbon $2p_\pi$ and

$2p_\sigma$ orbital, respectively, and θ is the angle between the Z axis and the vector connecting the C atom and the Na atom. For large C–Na distances, R, one can use the uniformly charged sphere[27,28] or the multipole expansion model[29] to evaluate these integrals. For $R>4$ Å these two models give results which differ by less than 1.5%. For small C–Na distances the semiempirical approach of Pariser and Parr[28] can be used, according to which the expressions for the integrals become

$$(\pi\pi \mid 3s3s) = \tfrac{1}{2}\{(\pi\pi \mid \pi\pi) + (3s3s \mid 3s3s)\} - a_\perp R^2 - b_\perp R, \tag{32a}$$

$$(\sigma\sigma \mid 3s3s) = \tfrac{1}{2}\{(\sigma\sigma \mid \sigma\sigma) + (3s3s \mid 3s3s)\} - a_{||} R^2 - b_{||} R, \tag{32b}$$

in which $a_\perp$, $b_\perp$, $a_{||}$, and $b_{||}$ are adjustable constants. The value of $(3s3s \mid 3s3s)$ can be calculated from the semiempirical expression[30]

$$(3s3s \mid 3s3s) = I_{Na} - E_{Na}$$

in which E_{Na} is the electron affinity of Na. Using values of 5.14 eV and 0 eV for I_{Na} and E_{Na}, respectively,[19,31] one finds

$$(3s3s \mid 3s3s) = 5.14 \text{ eV}.$$

Similarly, one finds[30]

$$(\sigma\sigma \mid \sigma\sigma) = (\pi\pi \mid \pi\pi) = 10.53 \text{ eV}.$$

For the actual calculations the uniformly charged sphere model was used for $R>6$ Å. For $R\leq6$ Å the Eqs. (32) were used. The parameters $a_\perp$, $b_\perp$, $a_{||}$, and $b_{||}$ were determined by calculating $(\pi\pi \mid 3s3s)$ and $(\sigma\sigma \mid 3s3s)$ with the uniformly charged sphere model for $R=6$ Å and $R=8$ Å and solving the Eqs. (32) for these parameters. The following values were calculated: $a_{||}=1.34$ eV/Å^2, $a_\perp=1.37$ eV/Å^2, $b_{||}=-7.4\times10^{-2}$ eV/Å, and $b_\perp=-7.7\times10^{-2}$ eV/Å.

D. ρ_0

The procedure for the calculation of the coefficients $c_{3s}{}^i$ and $c_i{}^{3s}$ outlined above proved to be unsatisfactory for the calculation of ρ_0 because the coefficient $\lambda_{6,3s}$ occurring in the expression (21) for ρ_0 became too large by an order of magnitude. This can be seen as follows. In the expression (22b) for $\lambda_{6,3s}$, the sum

$$\sum_{i=1}^{5} 2[ii \mid 6\,3s]$$

should have a value of about 1 eV in order to provide for a reasonable mixing of the excited state[2] $\Psi_{6,3s}$ with the zero-order ground state $^2\Psi_0$. This sum is approximately given by

$$\sum_{i=1}^{5} 2[ii \mid 6\,3s] \approx c_6{}^{3s} \sum_{i=1}^{5} 2[ii \mid 6\,6]^0 + c_{3s}{}^6 \sum_{i=1}^{5} 2[ii \mid 3s3s]^0. \tag{33}$$

It appears that the first sum in the right-hand side of this equation amounts to approximately 50 eV while the value of the second sum varies from 25 to 45 eV, depending upon the distance between the Na and the Nl ion. Since it follows from Eq. (28) that $c_{3s}{}^6 \approx -c_6{}^{3s}$, $\lambda_{6,3s}$ becomes large leading to a ground state with a considerable amount of CT character, and with a Na hfsc much larger than observed experimentally. One way to avoid this difficulty is to change the ratio of $c_{3s}{}^6$ and $c_6{}^{3s}$ by increasing $c_{3s}{}^6$ until the sums in Eq. (33) cancel. A more complete variational calculation than applied in our case might produce this result. However, theoretical zero order spin densities for the NaNl ion pair have been reported already in the literature by Goldberg and Bolton.[14] We have used these zero-order spin densities rather than changing arbitrarily the constants in the MO Φ_6 or Φ_{3s}. The values used for ρ_0 are given in Table IV.

E. Conversion Parameter

For the calculation of the Na hfsc one needs a parameter to convert $\mid \chi_{3s}(\mathbf{r}_N) \mid^2$ into gauss. The free atom value $A(3^2S)/\gamma_e\hbar = 316.081$ G (see Table I) could be used, but this value takes into account not only the direct contribution of the $3s$ electron to the spin density at the metal nucleus, but also the indirect contribution arising from the polarization of the metal core. The free atom value may therefore seem to be too large. However, one can show that the spin density, which in the ion pair is present in χ_{3s}, produces through higher order excitations core polarization in approximately the same proportion as a full electron does in the free atom. An example of this was given by the first sum in Eq. (13). The use of the free atom value, therefore, automatically accounts for the desired amount of core polarization. In our calculations the above given value of $A(3^2S)/\gamma_e\hbar$ was used.

F. Programs

Computations were performed on the Raytheon 706 computer of the Chemistry Department of the University of North Carolina at Chapel Hill. In addition, use was made of the facilities at the UNC computational center.

The formulas for the computation of the overlap integrals $S_{i,3s}$ and the formulas for the calculation of the repulsion integrals were incorporated in subroutines in the main program. The integrals $[ij \mid kl]^0$ were calculated with a separate routine.

IV. RESULTS AND DISCUSSION

In this section, the results of the calculations on the metal hfsc, a, in NaNl are presented and discussed. The contributions of various excitations to a are denoted by the same subscripts as the corresponding spin densities, e.g., $a_{1,8}$ corresponds to $\rho_{1,8}$ according to $a_{1,8} = 316.081 \times \rho_{1,8}$ G. For E_{3s}, a value of -3.84 eV was used, which is the energy of Φ_{3s} calculated for NaNl in DEE,

TABLE IV. Zero-order spin densities at the Na nucleus in NaNl for different positions of the cation in the XZ plane. Data taken from Ref. (14).

Y=0.0 Å, Z=0.0 Å				X=1.21 Å, Y=0.0 Å			
X(Å)	$\rho_0 \times 10^3$	X(Å)	$\rho_0 \times 10^3$	Z(Å)	$\rho_0 \times 10^3$	Z(Å)	$\rho_0 \times 10^3$
0.0	0.0	1.5	5.33	2.0	...	3.5	2.31
0.1	0.05	1.6	5.50	2.1	...	3.6	1.99
0.2	0.18	1.7	5.57	2.2	...	3.7	1.71
0.3	0.43	1.8	5.52	2.3	...	3.8	1.43
0.4	0.77	1.9	5.35	2.4	...	3.9	1.22
0.5	1.13	2.0	5.08	2.5	...	4.0	1.02
0.6	1.52	2.1	4.72	2.6	...	4.1	0.86
0.7	1.90	2.2	4.20	2.7	6.52	4.2	0.68
0.8	2.30	2.3	3.42	2.8	5.61	4.3	0.59
0.9	2.75	2.4	2.52	2.9	5.09	4.4	0.48
1.0	3.25	2.5	1.80	3.0	4.52	4.5	0.40
1.1	3.76	2.6	1.00	3.1	4.02	4.6	...
1.2	4.25	2.7	0.40	3.2	3.48	4.7	...
1.3	4.70	2.8	0.10	3.3	3.05	4.8	...
1.4	5.05	2.9	0.0	3.4	2.66	4.9	...

as explained in Sec. III. In addition, the variation of the first order contribution to the Na hfsc, a_1, with a variation of E_{3s} was investigated. E_{3s} was allowed to vary between -3.30 and -4.40 eV (see Sec. III).

The spin densities were calculated for the following positions of the Na ion:

(a) Positions above the center of one of the rings of Nl at $X=1.21$ Å, $Y=0.0$ Å, and $Z=0.0 \rightarrow 6.0$ Å were chosen to investigate the effect of an increase of the interionic distance on the metal hfsc.

(b) Positions along the Z axis at $X=0.0$ Å, $Y=0.0$ Å, and $Z=0.0 \rightarrow 6.0$ Å. These positions are of interest since the zero order spin density vanishes at these positions and the spin density will arise from higher order effects alone.

(c) Positions on an axis parallel to the X axis at $X=0.0 \rightarrow 6.0$ Å, $Y=0.0$ Å, and $Z=3.0$ Å. These positions were chosen to investigate the variation of the metal hfsc when the metal moves at constant height above the plane of the Nl ion.

The results are presented in the Figs. 2–4 and in Table V. To show the dependence of the different contributions to a_1 upon E_{3s}, detailed results are given for the positions mentioned above under (a). For the positions mentioned under (b) and (c), similar variations were found. Although spin densities for positions closer to the anion than 2 Å have probably no physical meaning,[6] they have been included for the sake of completeness.

The Figs. 2(a)–(d) represent values for a_{Ar} and $a_{Ar,M}$ for positions of the Na ion above the center of one of the rings of Nl, for four different energies E_{3s}. As an example, the contributions to a_{Ar} and $a_{Ar,M}$ from different excitations are given in Table V for $Z=2.5$ Å.

From the Figs. 2(a)–(d) it appears that $a_{Ar,M}$ usually gives by far the largest contribution to a_1. It was argued in Sec. II that this could be expected, since aromatic–metal excitations produce CT states in which there is a large spin density at the metal nucleus. Moreover, it was argued that $a_{Ar,M}$ probably would be negative, which is confirmed by the results presented in the Figs. 2(a)–(d). On the other hand, it appears from the same figures that a_{Ar} can be positive as well as negative and that its contribution to a_1 is small unless χ_{3s} is strongly admixed with a π MO of the aromatic ion. This occurs in our case for $E_{3s} = -3.84$ eV and -3.65 eV, which energies are close to the energy of -3.748 eV of the MO Φ_8. For instance, for $E_{3s} = -3.84$ eV, the admixture of χ_{3s} into Φ_8 may become as high as 30%–40% for a few positions of the metal ion. When this occurs

TABLE V. Contributions from different excitations to the metal hfsc in NaNl as a function of E_{3s}. The position of the alkali ion in this example is at $X=1.21$ Å, $Y=0.0$ Å and $Z=2.5$ Å, above the center of one of the rings of Nl.

	E_{3s}			
	-4.40 eV	-3.84 eV	-3.65 eV	-3.30 eV
$a_{1,8}$, gauss	-0.131	-0.637	0.532	0.095
$a_{4,8}$, gauss	0.065	0.302	-0.249	-0.043
a_{Ar}, gauss	-0.066	-0.335	0.283	0.052
$a_{1,3s}$, gauss	-0.617	0.130	-1.007	-0.486
$a_{2,3s}$, gauss	-0.285	-0.183	-0.161	-0.130
$a_{4,3s}$, gauss	-0.134	-0.346	0.220	0.018
$a_{Ar,M}$, gauss	-1.037	-0.398	-0.948	-0.598
a_1, gauss	-1.102	-0.733	-0.665	-0.546

the excitations $1 \rightarrow 8$ and $4 \rightarrow 8$ in fact correspond to excited states which have again a large amount of CT character, and it is not surprising that in these cases a_{Ar} gives a substantial contribution to a_1.
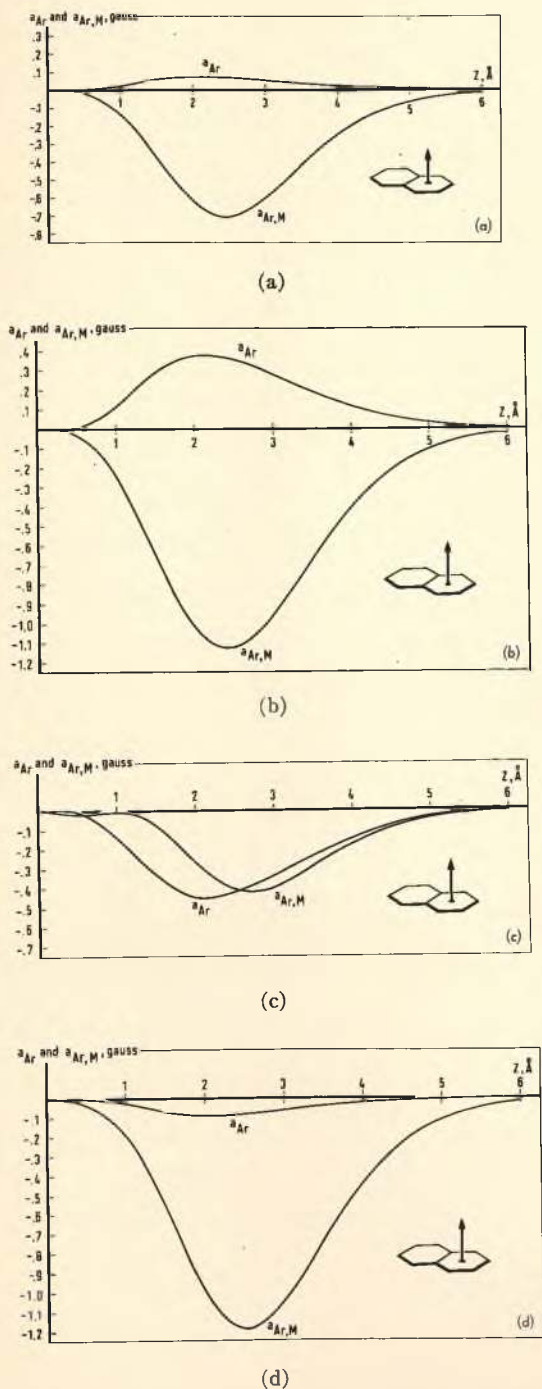

(a)

(b)

(c)

(d)

FIG. 2. Contributions to the Na hfsc in NaNl from local aromatic excitations, a_{Ar}, and from aromatic–metal cross excitations, $a_{Ar,M}$, vs the position of the Na ion above the center of one of the rings of the Nl ion ($X = 1.21$ Å, $Y = 0.0$ Å, and $Z = 0.0 \rightarrow 6.0$ Å), for $E_{3s} = -3.30$ eV (Fig. 2a), -3.65 eV (Fig. 2b), -3.84 eV (Fig. 2c), and -4.40 eV (Fig. 2d).
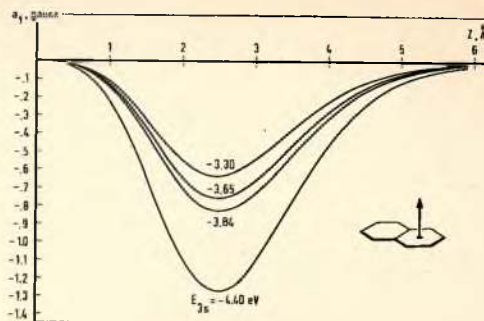

FIG. 3. First-order contribution, a_1, to the Na hfsc in NaNl vs the position of the Na ion above the center of one of the rings of the Nl ion ($X = 1.21$ Å, $Y = 0.0$ Å, and $Z = 0.0 \rightarrow 6.0$ Å), for $E_{3s} = -3.30$, -3.65, -3.84, and -4.40 eV.

In Fig. 3 the values of a_1 are presented for the same positions as in the Figs. 2. These data demonstrate that, although the contributions from various excitations to a_1 may vary strongly with a variation of E_{3s} (see Table V and Figs. 2), a_1 itself varies smoothly with E_{3s}. Even strong mixing of χ_{3s} with an antibonding MO of the aromatic ion does not affect this smooth dependence of a_1 upon E_{3s}. This may indicate that the different first-order excitations have probably been taken into account in a proper way in the calculations.

Finally, in the Figs. 4(a)–4(c) the values of the total hfsc for the positions mentioned above under (a), (b), and (c) are presented. From these figures it appears that in different regions of space the metal hfsc may have different signs and that, consequently, the sign of the metal hfsc may change with a change in the position of the cation. The data in the Figs. 4(a) and 4(c) show that in the region around the YZ plane, which is an antisymmetry plane of the first antibonding MO of Nl, the metal hfsc is negative. Around this region, a_0 is zero or very small and the total hfsc is nearly completely determined by the first-order contribution to the hfsc, a_1, which is negative. Figure 4(b) shows that, as the Na ion moves away from the plane of the aromatic ion, the metal hfsc may change sign and become negative before leveling off to zero, apparently because a_0 dies away faster with increasing interionic separation than a_1. A change in sign also occurs as the alkali ion moves away from the center of the molecule along the X axis as is clear from Fig. 4(c).

The results presented here allow a discussion of the dependence of the sign of the metal hfsc upon the atomic number of the alkali nucleus, Z_M, and the dependence of sign and magnitude of the metal hfsc upon the temperature (see the Introduction).

A. Dependence on Z_M

Three parameters may vary systematically with a systematic change in Z_M: the energy of the valence s AO of the metal, E_{ns}, the position of the alkali ion
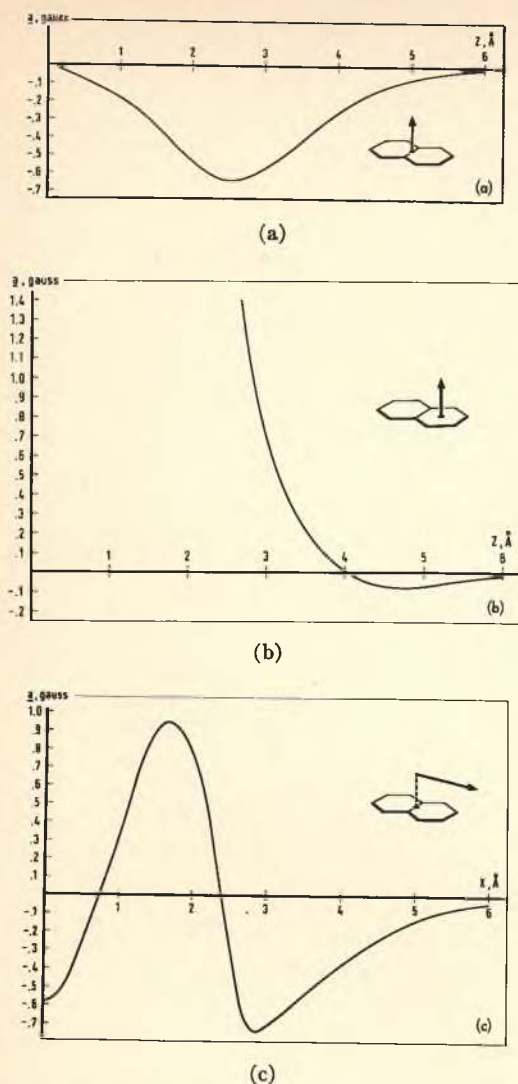
(a)

(b)

(c)

Fig. 4. (a) Na hfsc a in NaNl vs the position of the Na ion above the center of the Nl ion ($X=0.0$ Å, $Y=0.0$ Å, and $Z=0.0 \rightarrow 6.0$ Å), for $E_{3s}=-3.84$ eV; (b) Na hfsc a in NaNl vs the position of the Na ion above the center of one of the rings of the Nl ion ($X=1.21$ Å, $Y=0.0$ Å, and $Z=2.7 \rightarrow 6.0$ Å) for $E_{3s}=-3.85$ eV; (c) Na hfsc a in NaNl vs the position of the Na ion on an axis parallel to the X axis ($X=0.0 \rightarrow 6.0$ Å, $Y=0.0$ Å, $Z=3.0$ Å), for $E_{3s}=-3.84$ eV.

over the plane of the aromatic ion and the overlap integrals $S_{i,ns}$.

E_{ns} depends on the ionization potential of the alkali atom, which decreases regularly from Li to Cs. However, according to Eq. (27), E_{ns} will depend more on solvent and anion. Since the trend of the metal hfsc to become negative with increasing Z_M seems to be independent of solvent or aromatic ion, the change in E_{ns} with Z_M can probably not account for this trend.

A similar argument applies for the dependence of the sign on the position of the alkali ion. For the case of Nl, one might argue that for larger cations a position near the center of the anion, where there is a negative

spin density, is more likely than for smaller cations on account of Coulomb forces. Theoretical support for this assumption has been reported in the literature.[12,14] Although this reasoning may be valid for Nl, it is difficult to see how similar arguments would apply for any radical ion pair. Nevertheless, the change in sign from positive to negative with increasing Z_M has been observed for instance for ion pairs of naphthalene, anthracene, and biphenyl, and this trend seems to be independent of the anion. The dependence of the sign of the metal hfsc upon the position of the alkali ion can, therefore, probably not provide the explanation for the observed trend.

The third parameter on which the metal coupling constant depends is the overlap of χ_{ns} with the various MO's of the anion. The value of the overlap integral $S_{i,ns}$ depends on the number of nodes in the MO Φ_i^0 and upon the polarization of this MO by the alkali ion. As the number of nodes in Φ_i^0 increases, $S_{i,ns}$ will decrease and so, in general, $S_{i,ns}$ will be smaller for antibonding MO's than for bonding MO's. This is demonstrated by the data in Table VI, which gives the value of $S_{i,ns}$ for different MO's in a NaNl ion pair. On the other hand, electrostatic polarization of the π MO's may affect the values of $S_{i,ns}$ appreciably.[14,32] This effect is characteristic for the alkali ion and is important mainly for the smaller ions like Li$^+$ and Na$^+$. For instance, for NaNl polarization of Φ_6^0 may increase $S_{6,3s}$ almost by an order of magnitude.[14] It may also be expected that the overlap of χ_{ns} with antibonding MO's is more sensitive towards polarization effects than the overlap with bonding MO's: overlap with bonding MO's will usually be large regardless whether or not polarization effects are taken into account. It can be concluded that for small cations $S_{i,ns}$ will be large for both bonding and antibonding MO's Φ_i^0, while for large cations $S_{i,ns}$ will be large for the bonding MO's, especially the lower ones, and small for the antibonding MO's.

The zero- and first-order contribution to the metal hfsc depend differently on these overlap integrals. a_0 depends on the overlap of χ_{ns} with the *first anti-*

TABLE VI. Values of the overlap integral $S_{i,3s}$ of χ_{3s} with different Hückel MO's Φ_i^0 of Nl for different positions of the Na ion above the center of one of the rings of Nl. No polarization of the MO's was taken into account.

| MO | $X=1.21$ Å, $Y=0.0$ Å $Z=$ | | | | |
	2.0 Å	2.5 Å	3.0 Å	3.5 Å	4.0 Å
1	0.206	0.218	0.201	0.168	0.130
2	−0.064	−0.073	−0.069	−0.057	−0.044
4	0.022	0.022	0.020	0.017	0.013
6	−0.002	0.001	0.002	0.001	0.001
8	−0.011	−0.009	−0.007	−0.006	−0.005

bonding MO, while a_1 depends by means of the aromatic–metal cross excitations mainly upon the overlap of χ_{ns} with the *bonding* MO's of the anion. The preceding argument, therefore, shows that with an increase in the size of the cation the contribution of a_1 to the total hfsc will gain importance over a_0. Since a_1 can be expected to be negative, whereas a_0 is always positive, the total hfcs will show a tendency to become more negative if the size of the alkali ion increases. Further calculations and experiments have to be performed to test this explanation.

B. Dependence Upon the Temperature

It was mentioned in the Introduction that three models have been proposed in the literature to explain the temperature dependence of the metal hfsc in alkali radical ion pairs: the vibrational model of Atherton and Weissman, the equilibrium model of Hirota and Kreilick, and Hogen-Esch and Smid, and the static model of Chang, Slates, and Swarc. Their implications will be discussed briefly in the following on the basis of the results presented in this section.

Aono and Oohashi, using the vibrational model,[12] calculated that from 200 to 300°K the root-mean-square amplitude of the vibration of the Na ion in a NaNl ion pair would increase by approximately 0.2 Å. According to Fig. 4(c), this would correspond with a slope of the a vs T curve of about 0.1–0.3 G/100°C. This is of the same order of magnitude as the slope observed for instance for NaNl in 2-methyltetrahydrofuran (0.4 g/100°C'), but it is appreciably lower than the slope observed for instance for NaNl in tetrahydrofuran (THF).[1] Further, the limited experimental evidence available until now seems to indicate that, whenever a change in sign occurs with a change in temperature the change is from positive to negative with decreasing temperature.[4,6,8] There is no general way to explain this by invoking the vibrational model, although for the special case of an alkali Nl ion pair the vibrational model could account for such a change in sign, as Fig. 4(c) shows, provided the minimum in the potential energy well of the cation is over the 9–10 bond of Nl.

The equilibrium model explains in a natural way the large slope in the a vs T plot measured for NaNl in THF on the assumption that there exists a temperature dependent equilibrium between contact and solvent separated ion pairs. The existence of solvent separated ion pairs accounts for the observation that the metal hfsc may be zero even if ion pairing occurs, which is difficult to explain on the basis of the vibrational model. Figures 4 show that for the Na hfsc to be zero, the interionic distance in the ion pair must be of the order of 4–6 Å which is consistent with the idea that solvent molecules actually separate the ions. The equilibrium model does not explain the occurrence of a change in sign of the metal hfsc with temperature nor

the occurrence of positive and negative slopes in the same a vs T curve at different temperatures as was observed for instance for Cs biphenyl ion pairs.[5]

The static model relates the temperature dependence of the metal hfsc to the change in the solvation of the alkali ion with temperature. As the solvation changes, the position of the cation over the plane of the anion as well as the distance to this plane may vary and Figs. 4 show that the sign of the metal hfsc as well as the sign of the slope of the a vs T curve may change then. Especially towards lower temperatures, as the solvation of the cation increases, the distance between alkali ion and anion will increase which may result in a change in sign of the metal hfsc from positive to negative as Fig. 4(b) shows. This can be related again to the polarizing influence of the cation: as the interionic distance increases, polarization effects will decrease, which causes a_0 to fall off more rapidly than a_1. Since the latter can be expected to be negative and a_0 is always positive, the total coupling constant may show a tendency to become negative at low temperatures.

It can be concluded that, using a combination of the vibrational model and the equilibrium or the static model, one can probably in most cases account for the variation of the metal hfsc with temperature.

Finally, it is remarked that an experimental check of the calculations is not possible as long as the position of the Na ion in the NaNl ion pair has not been established experimentally. The results presented here combined with the observation that the sign of the Na hfsc in NaNl is positive[8] seem to indicate that the position of the Na ion is above one of the rings of the Nl molecule, for which conclusion there is theoretical evidence.[12,14] Hopefully, experiments on single crystals of alkali radical ion pairs may provide more insight in the structure of these ion pairs.[33]

V. CONCLUSION

The results presented in the preceding section show that the procedure used for the calculation of the first-order spin density gives results of the correct order of magnitude. The difficulties experienced with the calculation of the zero order spin density can possibly be avoided by using an improved variational procedure. The calculations have clearly demonstrated that for an estimate of the total spin density at the metal nucleus, it is not sufficient to calculate the zero order spin density alone: the first-order contribution to the spin density is often of the same order of magnitude and will usually have a different sign. Most important seems to be the conclusion that the metal hfsc may have different signs in different regions of space. Particularly where there is an antisymmetry plane in the first antibonding MO of the aromatic ion, a region of negative spin density will occur. The observation that the metal hfsc has a tendency to become negative with increasing atomic number of the alkali nucleus was related to the

polarizing power of the alkali ions: electrostatic polarization of the π MO's enhances the zero-order spin density compared to the first-order spin density. Thus, going from small, strongly polarizing ions to large, weakly polarizing ions the total spin density will increasingly be determined by the first-order, negative, spin density and thus show a tendency to become negative. This explanation can be checked by performing calculations on Rb-radical ion pairs. The change in sign of the metal hfsc observed for some systems upon a lowering of the temperature could be explained on the basis of either the vibrational model of Atherton and Weissman or the static model. In general, by combining the features of the vibrational model with those of the equilibrium model or the static model one will be able to explain the temperature dependence of the metal hfsc in most cases. It is pointed out, however, that for a shallow potential energy well of the alkali ion in the ion pair the distinction between the vibrational and the equilibrium model may become meaningless.

ACKNOWLEDGMENT

G. W. Canters thanks Professor C. S. Johnson, Jr. for the critical reading of the manuscript and for permission to use the computer of the Chemistry Department of the University of North Carolina at Chapel Hill. He thanks Professor L. Pedersen for useful suggestions and comments. The authors are grateful to Dr. I. B. Goldberg and Professor J. R. Bolton and to Professor L. Pedersen and Dr. R. G. Griffin for sending preprints of their papers.

APPENDIX

In the following, it is shown how the value of the spin density at the nucleus in a free alkali atom can be obtained from spectroscopic data. For the analysis the theory for the hyperfine structure in atomic spectra will be used.[34] For our purposes we consider the fine structure terms $n^2S_{1/2}$, $n^2P_{1/2}$, and $n^2P_{3/2}$, in which the unpaired electron is present in the valence ns orbital (n^2S) or the valence np orbital (n^2P), respectively. The fine structure levels are split by the hyperfine interaction between the total angular momentum $\mathbf{J}=\mathbf{L}+\mathbf{S}$ and the magnetic moment of the nucleus, where $\mathbf{L}$ represents the orbital angular momentum and $\mathbf{S}$ the electron spin angular momentum. The energy of each hyperfine level depends only on the total spin $\mathbf{F}$, given by $\mathbf{F}=\mathbf{J}+\mathbf{I}$, where $\mathbf{I}$ is the nuclear spin angular momentum.

The distance W_F of the hfs levels, belonging to a particular term, to the center of gravity of this term is given, in energy units, by[34]

$$W_F = (A/2)C + B\frac{3/2C(C+1) - 2I(I+1)J(J+1)}{2I(I+1)2J(J+1)}$$

$$\text{(A1)}$$

in which $C = F(F+1) - I(I+1) - J(J+1)$. A and B characterize, respectively, the magnetic and the quadrupole interaction between the nucleus and the electrons of the atom (for $J \leq \frac{1}{2}$, $B = 0$).

The magnetic constants pertaining to our problem, are denoted by $A(n^2S)$, $a_{1/2}$ and $a_{3/2}$ for the terms $n^2S_{1/2}$, $n^2P_{1/2}$, and $n^2P_{3/2}$, respectively. Thus, for the energy difference between the two hyperfine levels with $F = I + \frac{1}{2}$ and $F = I - \frac{1}{2}$ of the term $n^2S_{1/2}$, one finds, using Eq. (A1),

$$W_{I+1/2} - W_{I-1/2} = \frac{1}{2}A(n^2S) \times (2I+1).\quad \text{(A2)}$$

For the energy differences between the hfs levels of the other terms, similar equations hold. Thus, from a knowledge of the energy differences between the hfs levels, the constants $A(n^2S)$, $a_{1/2}$, and $a_{3/2}$ can be determined.

In general, there are three interactions that contribute to the magnetic constant:

(a) the Fermi contact (Fc) interaction,

(b) the interaction between the nuclear magnetic moment and the orbital momentum of the electrons,

(c) the magnetic point dipole interaction between the nuclear spin and the electron spin.

$A(n^2S)$ is only determined by the Fc interaction and is given by

$$A(n^2S) = (8\pi/3)\gamma_e\gamma_N\hbar^2\rho(n^2S),\quad \text{(A3)}$$

in which $\rho(n^2S)$ is the spin density at the metal nucleus in the n^2S state of the free atom. Eq. (A3) has a form analogous to that of Eq. (14). $A(n^2S)$ can be obtained directly from Eq. (A2). Values of $A(n^2S)$ for different alkali isotopes have been given in Table I.

All three above mentioned interactions contribute to $a_{1/2}$ and $a_{3/2}$. The contributions of the Fc interaction are usually denoted by $a_{c,1/2}$ and $a_{c,3/2}$, while the sums of the other two contributions are usually denoted by $a_{d,1/2}$ and $a_{d,3/2}$. Thus,

$$a_{1/2} = a_{c,1/2} + a_{d,1/2},\quad \text{(A4a)}$$

$$a_{3/2} = a_{c,3/2} + a_{d,3/2}.\quad \text{(A4b)}$$

If volume and relativistic corrections are neglected,[34] the following relations hold between $a_{c,1/2}$, $a_{c,3/2}$, $a_{d,1/2}$, and $a_{d,3/2}$[17]:

$$a_{c,1/2} = -a_{c,3/2},\quad \text{(A5a)}$$

$$a_{d,1/2} = 5a_{d,3/2}.\quad \text{(A5b)}$$

Since $a_{c,3/2}$ is given by[17]

$$a_{c,3/2} = (8\pi/9)\gamma_e\gamma_N\hbar^2\rho(n^2P),\quad \text{(A6)}$$

one obtains from the Eqs. (14) and (A4)–(A6)

$$A(n^2P) = \frac{1}{2}(5a_{3/2} - a_{1/2}).\quad \text{(A7)}$$

With the help of this equation, $A(n^2P)$ can be calculated from the values of $a_{3/2}$ and $a_{1/2}$ obtained from op-

tical double resonance, atomic beam, and level crossing experiments.

The validity of Eq. (A5b) has been questioned in the literature. Lyons et al.[35] have argued that this equation is strictly valid only for a single particle approach and that the correct value for the constant in this equation is expected to differ from 5. By using Brueckner–Goldstone many-body theory, they showed that for Li the ratio of $a_{d,1/2}$ and $a_{d,3/2}$ is equal to 5.35 and that the value of $A(n^2P)$ for Li equals -28.7 Mc/sec instead of -31.6 Mc/sec, as calculated from Eq. (A7). They indicated a high accuracy for their result (1.5%) which seems to be granted by the success of the many body theory in predicting the hfs constants for Li and other atoms.[35,36] Svanberg and Rydberg[37] calculated for Cs a value of 6.95 instead of 5 for the proportionality constant in Eq. (A5b), which changes $A(n^2P)$ for Cs^{133} from -13 Mc/sec, as calculated from Eq. (A7), to $+28$ Mc/sec. For Na, K, and Rb, however, Eq. (A7) had to be used since the correct value of the proportionality constant in Eq. (A5b) is not known for these elements. As in the case of Cs, the use of the correct value would probably result in larger values of $A(n^2P)$. The changes, however, can be expected to be not so large as to invalidate the discussion of the local metal excitations given in Sec. II.

The values of $A(n^2P)$ have been given for different alkali isotopes in Table I. For Na and K the sign of $A(n^2P)$ is uncertain. This is because for these metals $A(n^2P)$, as calculated from Eq. (A7), is of the same order of magnitude as the reported errors in the constants $a_{1/2}$ and $a_{3/2}$.

* Supported in part by a grant from the UNC Materials Research Center (Contract SD-100 with the Advanced Research Projects Agency).

† NATO postdoctoral fellow 1968–1969.

‡ Present address: Institute for Physical Chemistry, University of Padua, Padua, Italy.

[1] N. M. Atherton and S. I. Weissmann, J. Am. Chem. Soc. 83, 1330 (1961).

[2] E. de Boer, Rec. Trav. Chim. 84, 609 (1965).

[3] N. Hirota, J. Am. Chem. Soc. 89, 32 (1967); P. Graceffa and T. R. Tuttle, Jr., J. Chem. Phys. 50, 1908 (1969); M. Komarynski, thesis, Washington University, 1968.

[4] G. W. Canters, E. de Boer, B. M. P. Hendriks, and H. van Willigen, Chem. Phys. Letters 1, 627 (1968).

[5] G. W. Canters, E. de Boer, B. M. P. Hendriks, and A. A. K. Klaassen, Proc. Colloq. AMPÈRE. Atomes Mol. Etudes Radio Elec. 15, 242 (1969).

[6] G. W. Canters, thesis, Nijmegen University, Nijmegen, The Netherlands, 1969.

[7] T. Takeshita and N. Hirota, Chem. Phys. Letters 4, 369 (1969).

[8] B. M. P. Hendriks, G. W. Canters, C. Corvaja, J. W. M. de Boer, and E. de Boer, Mol. Phys. (to be published).

[9] N. Hirota, J. Am. Chem. Soc. 90, 3603 (1968); C. L. Dodson and A. H. Reddoch, J. Chem. Phys. 48, 3226 (1968); E. Warhurst and A. M. Wilde, Trans. Faraday Soc. 65, 1413 (1969).

[10] S. Winstein, E. Clippinger, A. H. Fainberg, and G. C. Robinson, J. Am. Chem. Soc. 76, 2597 (1954); S. Winstein and G. C. Robinson, ibid. 80, 169 (1958); E. Grunwald, Anal. Chem. 26, 1696 (1954).

[11] (a) N. Hirota and R. W. Kreilick, J. Am. Chem. Soc. 88, 614, 1966; (b) T. E. Hogen-Esch and J. Smid, ibid. 88, 307 (1966); (c) P. Chang, R. V. Slates, and M. Szwarc, J. Phys. Chem. 70, 3180 (1966).

[12] S. Aono and K. Oohashi, Progr. Theoret. Phys. (Kyoto) 30, 162 (1963); 32, 1 (1964).

[13] L. Pedersen and R. G. Griffin, Chem. Phys. Letters 5, 373 (1970).

[14] I. B. Goldberg and J. R. Bolton, J. Phys. Chem. 74, 1965 (1970).

[15] M. C. R. Symons, Nature 224, 685 (1969).

[16] H. M. McConnell, J. Chem. Phys. 28, 1188 (1958).

[17] D. A. Goodings, Phys. Rev. 123, 1706 (1961).

[18] C. P. Slichter, Principles of Magnetic Resonance (Harper and Row, New York, 1963), Sec. 4.6.

[19] G. Herzberg, Atomic Spectra and Atomic Structure (Dover, New York, 1944), Chap. 6.

[20] R. Pariser, J. Chem. Phys. 24, 250 (1956).

[21] A. Streitweiser, Jr., Molecular Orbital Theory for Organic Chemists (Wiley, New York, 1961), Chap. 7.

[22] A. I. Shatenshtein and E. S. Petrov, Russ. Chem. Rev. English Transl. 36, 100 (1967).

[23] A. I. Shatenshtein, M. I. Belousova, and E. S. Petrov, Dokl. Academia Nauk SSSR, 161, 889 (1965).

[24] C. A. Coulson, Valence (Oxford U. P., Oxford, England, 1961), Chap. 4.

[25] R. S. Mulliken, C. A. Rieke, D. Orloff, and H. Orloff, J. Chem. Phys. 17, 1248 (1949).

[26] M. Wolfsberg and L. Helmholz, J. Chem. Phys. 20, 837 (1952); C. J. Ballhausen and H. B. Gray, Molecular Orbital Theory (New York, 1964), p. 118.

[27] R. G. Parr, J. Chem. Phys. 20, 1499 (1952).

[28] R. Pariser and R. G. Parr, J. Chem. Phys. 21, 466, 767 (1953).

[29] R. G. Parr, J. Chem. Phys. 33, 1184 (1960).

[30] R. Pariser, J. Chem. Phys. 21, 568 (1953).

[31] L. Pauling, The Nature of the Chemical Bond (Cornell U. P., Ithaca, New York, 1960), Chap. 3.

[32] B. J. McClelland, Trans. Faraday Soc. 57, 1459 (1961).

[33] G. W. Canters, A. A. K. Klaassen, and E. de Boer, J. Phys. Chem. 74, 3299 (1970).

[34] H. G. Kuhn, Atomic Spectra (Academic, New York, 1962), Chap. 6; H. Kopfermann, Nuclear Moments (Academic, New York, 1958); G. Herzberg, Atomic Spectra (Academic, New York, 1962), Chap. 1–4.

[35] J. D. Lyons, R. T. Pu, and T. P. Das, Phys. Rev. 178, 103 (1969).

[36] E. S. Chang, R. T. Pu, and T. P. Das, Phys. Rev. 174, 1, 16 (1968); N. C. Dutta, C. Matsubura, R. T. Pu, and T. P. Das, Phys. Rev. Letters 21, 1139 (1968); Phys. Rev. 177, 33 (1969).

[37] S. Svanberg and S. Rydberg, Z. Physik 227, 216 (1969).